The Seventh Asian-Pacific Symposium on Structural Reliability and Its Applications (APSSRA2020)
October 4–7 2020, Tokyo, Japan
T. Takada, I. Yoshida & T. Itoi (editors)

Identification of consolidation parameters of Ma12 layer in Osaka Bay through data assimilation

K. Oda[1]

[1]*Osaka Sangyo University. Email: oda@ce.osaka-sandai.ac.jp*

Abstract: Several man-made islands have been constructed in Osaka Bay. Their consolidation behaviors should be predicted to maintain and manage the facilities and infrastructures located on the islands. However, it is difficult to predict their consolidation settlements accurately before their construction. Therefore, it is desirable to predict their settlement behaviors in the future through field measurements from the commencement of the construction. Data assimilation methods have been extensively used in various scientific fields within the past few years. Such methods are used to identify the simulation model through which a reasonable prediction can be performed by correcting a simulation according to field measurements. In this study, the particle filter method, which is a data assimilation technique, was applied to identify the simulation model for reproducing the consolidation behavior of the Ma12 layer, which is the upper Pleistocene clay layer in Osaka Bay. First, numerical analysis was conducted for reproducing the consolidation behavior of Ma12, including application of the particle filter method. A compression curve as conventional as possible was adopted for use in the numerical analysis. Then, the analysis model was established by considering the positions of pore water pressure meters installed within the Ma12 layer. Moreover, the consolidation parameters before data assimilation were determined based on the results of the soil tests. Finally, the applicability of the identified analytical model was assessed by comparing the field measurements and analytical results of both consolidation settlement and pore water pressures.

Keywords: data assimilation, particle filter, consolidation, soil properties, Pleistocene clay.

1. Introduction

The seabed ground of Osaka Bay in Japan is composed of thick clay layers and sandy gravel layers, which accumulate alternately. The formation of 14 thick marine clay layers (Ma0–Ma13) was established through geological research studies. Ma13 is the uppermost layer near the seabed; it has a Holocene origin, whereas the other clay layers, i.e., Ma12–Ma0, have a Pleistocene origin. Therefore, a significant consolidation settlement of clay layers occurred during the construction of man-made islands in Osaka Bay. Accurate estimation of the consolidation settlement is necessary to formulate a management plan for facilities and infrastructures in these islands.

The Pleistocene clays in Osaka Bay are referred to as “quasi-overconsolidated clays.” Their consolidation behavior is notably distinct from that of overconsolidated clays owing to their loading and unloading histories (Mimura et al., 2003). Moreover, the in-situ consolidation behavior is different from that obtained through consolidation tests, such as oedometer tests, which are performed in the laboratory, because of various factors such as differences in the strain rate of the consolidation process (Tanaka, 2005); (Watabe et al., 2008). Therefore, it is difficult to estimate the consolidation settlement of the man-made islands in Osaka Bay based on consolidation properties derived from consolidation tests in the laboratory.

Historically, data assimilation techniques were developed for applications, such as weather forecasting and maritime weather prediction. Recently, their application scope has been broadened to include geotechnical problems. For example, the identification of analytical models for rainwater infiltration into the ground (Ito et al., 2016) and the estimation of the stability of a natural slope (Futatsugi et al., 2018) were reported. Moreover, finite element (FE) analysis using the particle filter method was applied for the estimation of the deformation behavior of a Holocene clay layer for the construction of a large-scale man-made island (Shuku et al., 2010; Shibata et al., 2019).

In this study, the applicability of data assimilation was analyzed to identify the simulation model for reproducing the consolidation behavior of the Ma12 layer. The numerical analysis and analytical model were studied from the viewpoint of practical application. Finally, the availability of the identified analytical model was assessed by comparing the field measurements and analytical results of both the consolidation settlement and pore water pressures.

2. Data Assimilation Analyses

The particle filter method is a sequential data assimilation

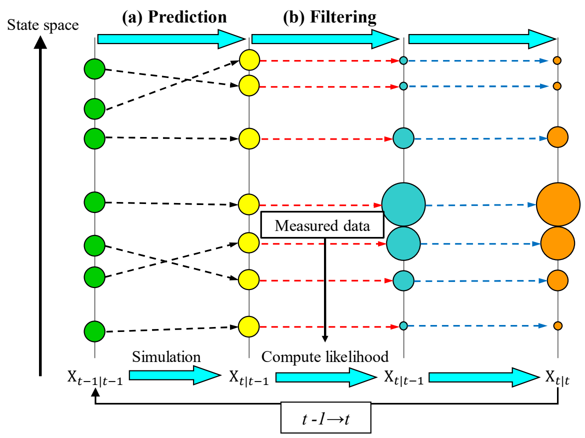

Figure 1. Schematic of computational procedure for particle filter method.

method in which the probability distribution of a physical quantity is approximated with its realizations. Each realization is referred to as a particle, and each set is called an ensemble. A particle filter method determines the number of particles at a discrete time using Bayes' theorem. Figure 1 shows the computational procedure of a particle filter method. First, numerous numerical simulations are performed in which different sets of soil characteristics are applied for each particle (prediction part (a) in Fig.1). Subsequently, the likelihood of each particle is evaluated by comparing the measured and simulated data (filtering part (b) in Fig. 1). Based on the particle filter method, the particles with higher compatibility with the field observations can be retained through iteration over these two steps.

In this study, the particle filter method was applied to conduct an inverse analysis (Murakaki et al., 2013). Thus, the system and observation models were formulated using Eqs. (1) and (2).

$$x_t = f_t\left(x_{t-1}\right) + v_t \tag{1}$$

$$y_t = h_t\left(x_t\right) + w_t \tag{2}$$

Equation (1) is the system model, whereas Eq. (2) is the observation model. Vector x_t is the state vector, which includes the physical quantity at a discrete time (t = 1, 2, …, T). Vector y_t is the observation vector, which includes the field observations. A set of unknown soil characteristics (k, Cc, and OCR) is additionally incorporated into the state vector. Vectors v_t and w_t represent the system noise and observation noise, respectively. The nonlinear function h_t is the observation matrix; it is composed of either zeros or ones. The operator f_t denotes the evolution of the settlement from t-1 to t, based on the simulation model.

A data assimilation strategy based on the particle filter method employs an ensemble approximation technique, where a probabilistic density function of stochastic variables is approximated with its realizations. For example, the filtered distribution $p(x_{t-1}|y_{1:t-1})$ at time t-1 is approximated by the ensemble $\{x^{(1)}_{t-1|t-1}, x^{(2)}_{t-1|t-1}, \ldots, x^{(N)}_{t-1|t-1}\}$ according to the following equation:

$$p\left(x_{t-1}\middle|y_{1:t-1}\right) \approx \frac{1}{N}\sum_{i=1}^{N}\delta\left(x_{t-1} - x^{(i)}_{t-1|t-1}\right) \tag{3}$$

where δ is Dirac's delta function, and N is the number of particles in the ensemble.

We obtain the ensemble approximation for the predicted distribution $p(x_t|y_{1:t-1})$ at time t from the filtered ensemble at time t-1, according to the following equation:

$$\begin{aligned} p\left(x_t\middle|y_{1:t-1}\right) &= \int p\left(x_{t-1}\middle|y_{1:t-1}\right)p\left(x_t\middle|x_{t-1}\right)dx_{t-1} \\ &\approx \frac{1}{N}\sum_{i=1}^{N}\int\delta\left(x_{t-1} - x^{(i)}_{t-1|t-1}\right)p\left(x_t\middle|x_{t-1}\right)dx_{t-1} \\ &= \frac{1}{N}\sum_{i=1}^{N}\delta\left(x_t - \left(f_t\left(x^{(i)}_{t-1|t-1}\right) + v^{(i)}_t\right)\right) \\ &= \frac{1}{N}\sum_{i=1}^{N}\delta\left(x_t - x^{(i)}_{t|t-1}\right), \end{aligned} \tag{4}$$

where $\{v^{(i)}_t\}^{N}_{i=1}$ is an independent and identically distributed sample set. This calculation indicates that each particle of the prediction ensemble is generated using the state equation.

We obtain an approximation of the filtered distribution $p(x_t|y_{1:t})$ from the ensemble of the predicted distribution $p(x_t|y_{1:t-1})$, and the observation vector y_t using Bayes' theorem is expressed as follows:

$$\begin{aligned} p\left(x_t\middle|y_{1:t}\right) &= \frac{p\left(y_t\middle|x_t\right)p\left(x_t\middle|y_{1:t-1}\right)}{\int p\left(y_t\middle|x_t\right)p\left(x_t\middle|y_{1:t-1}\right)dx_t} \\ &\approx \frac{p\left(y_t\middle|x^{(i)}_{t|t-1}\right)p\left(x^{(i)}_{t|t-1}\middle|y_{1:t-1}\right)}{\sum_{i=1}^{N}p\left(y_t\middle|x^{(i)}_{t|t-1}\right)p\left(x^{(i)}_{t|t-1}\middle|y_{1:t-1}\right)} \\ &= \frac{s^{(i)}_t\cdot\frac{1}{N}}{\sum_{i=1}^{N}s^{(i)}_t\cdot\frac{1}{N}} \\ &= \frac{s^{(i)}_t}{\sum_{i=1}^{N}s^{(i)}_t} \end{aligned} \tag{5}$$

where $s^{(i)}_t$ is defined as follows.

$$s^{(i)}_t = p\left(y_t\middle|x^{(i)}_{t|t-1}\right) \tag{6}$$

The likelihood of $s^{(i)}_t$ occurring in the case of linear observations is determined using the following equation:

$$\begin{aligned} &p\left(y_t\middle|x^{(i)}_{t|t-1}\right) = \\ &\frac{1}{\sqrt{2\pi}^{m}|R|}\exp\left[\frac{-\left\{y_t - h\left(x^{(i)}_{t|t-1}\right)\right\}^{T}R^{-1}\left\{y_t - h\left(x^{(i)}_{t|t-1}\right)\right\}}{2}\right] \end{aligned} \tag{7}$$

where m is the number of observation points, and R is the variance-covariance matrix.

3. Simulation Model

In this study, a soil-water coupling FE analysis (Akai et al., 1978) was employed as the simulation model. In particular, a one-dimensional analysis was applied. Figure 2 shows a conceptual diagram of the compression curve used in this study. A one-dimensional consolidation state is assumed in this model, so that the conventional model, which is composed of two straight lines, can be applied. Ignoring the settlement in the over-consolidated state, in which the current stress is less than the consolidation yield stress, i.e., pc, it is required to identify the compression index, Cc, and pc. Cc is an index that governs the compressibility of clays, and it is defined as the slope of the compression curve in the normally consolidated state. In contrast, pc is the compressive stress at which the compressibility increases. This phenomenon is equivalent to material yielding. Moreover, the coefficient of permeability, k, which significantly influences the consolidation rate, must be

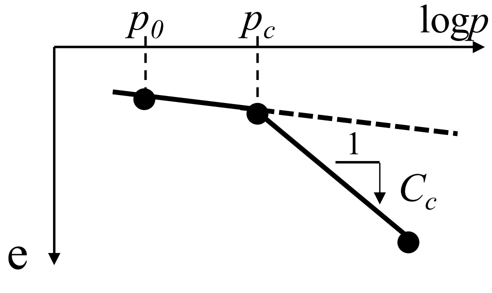

Figure 2. Conceptual diagram of compression curve.

identified. These three consolidation parameters, i.e., *Cc*, *pc,* and *k*, are usually determined through consolidation tests performed in the laboratory.

4. Monitoring Site

Figure 3 shows the location of the monitoring site. Kobe Airport was chosen as the research target because the field measurements of settlements and pore water pressures were already available (Hasegawa et al. 2006). Kobe Airport is located in the northern part of Osaka Bay, and it was constructed at the farthest location off Kobe. The increase in the overburden pressure owing to the construction is approximately 400 kPa, affecting the deeper part of the ground. Therefore, the estimation of the consolidation settlement of the Pleistocene clay layers is a critical engineering issue. The measurements of settlement at several positions in the ground have been still carried out.

Figure 3(a). Location of Kobe Airport.

Figure 3(b). Location of monitoring site in Kobe Airport.

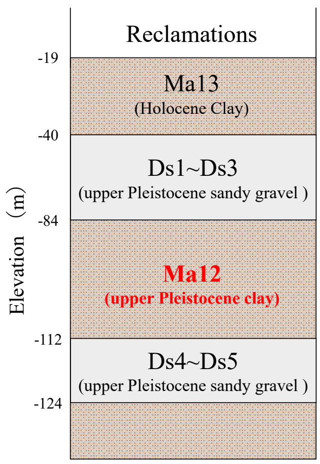

Figure 4. Schematic view of stratums at monitoring site.

Figure 4 shows the schematic view of strata at the monitoring site. In this study, the author analyzed the Ma12 layer, which is composed of the upper Pleistocene clay, because the largest consolidation settlement occurs in the Ma12 layer. Moreover, this layer is thick and cannot be improved by sand drains and so on. Consequently, its consolidation occurs very slowly.

5. Analytical Model of Ma12 Layer

Figure 5 shows the one-dimensional analytical model with the positions of the measurement devices. The red circle on the analysis model denotes a settlement gauge. Another settlement gauge was installed at the top of the Ma11 clay layer. The difference between the two settlements can be considered as the consolidation settlement of only the Ma12 clay layer because the settlement of sand mixed with a gravel layer between the Ma12 layer and the Ma11 layer can be ignored. By contrast, the blue circles denote pore water pressure meters. The progress of consolidation of the Ma12 layer can be estimated in detail through the eight pore water pressures measured.

Figure 6 shows the vertical distribution of the consolidation parameters. The points denote the results of the consolidation tests. The undisturbed samples that were collected near the monitoring site were used for the consolidation tests. The solid lines are the representative values for each parameter. These lines were determined by spatial interpolation through artificial intelligence. The two dotted lines shown in Figs. 6(a) and (b) indicate the maximum and minimum values in the data assimilation, respectively. The maximum value was obtained by adding the standard deviation to the representative value, whereas the minimum value was obtained by subtracting the standard deviation to the representative value. The consolidation parameters for each particle were determined within the range from the minimum to the maximum. However, they were not determined randomly. The vertical distribution trend of the consolidation parameters at each particle was set in agreement with that of their representative values. Consequently, the difference between the consolidation parameters at each particle and those at the representative values was randomly changed. In contrast, the maximum value of *pc* corresponded to that of the representative value, because it is empirically established that the value of *pc* in situ does not exceed that of consolidation tests. Moreover, the minimum value of *pc* corresponded to p_0, i.e., overburden pressure. Finally, *pc* at each particle was determined by randomly varying the *pc* to p_0 ratio.

6. Data Assimilation

Figure 7 shows the history of surcharge owing to reclamation. The numerical simulations were carried out from 2000 through 2014. However, the data assimilation was applied

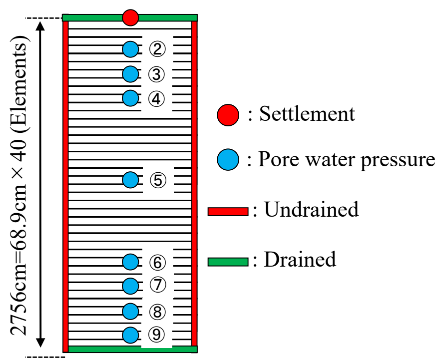

Figure 5. Analytical model.

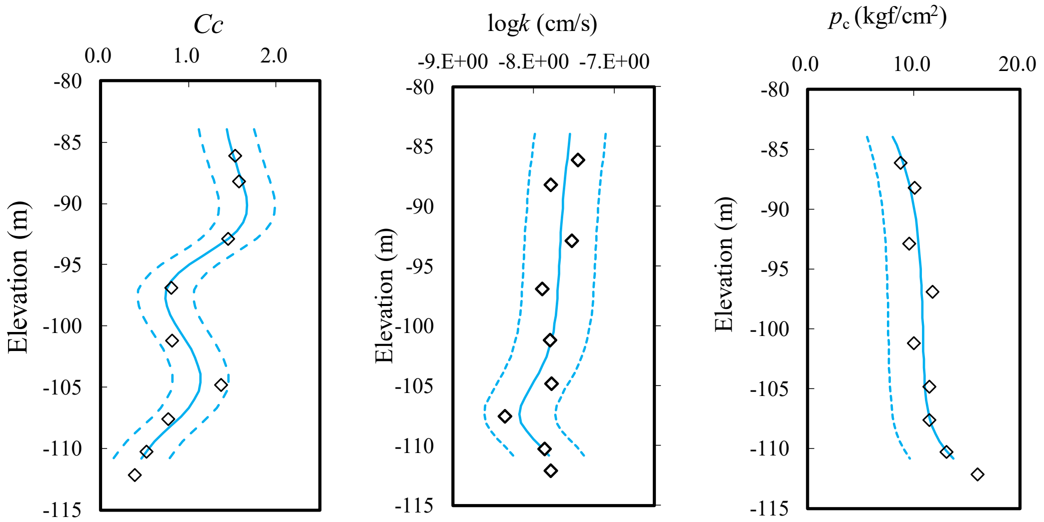

(a) Compression index (b) Coefficient of permeability (c) Consolidation yield stress

Figure 6. Vertical distribution of consolidation parameters.

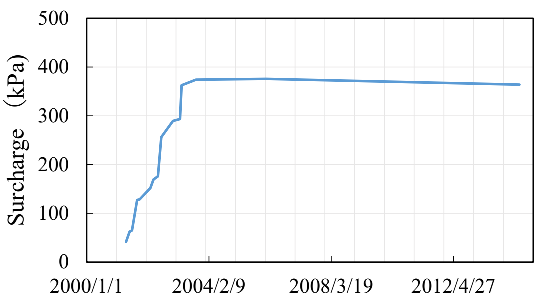

Figure 7. History of surcharge owing to reclamation.

from 2006 to 2014 because the pore water pressures at all the measurement positions started dissipating since approximately 2006. A total of 100 particles were used for data assimilation. In addition, the standard deviations of observation noise were 5 cm and 29.0 kPa for the settlement and pore water pressure, respectively.

Figure 8 shows a comparison between the field measurements and data assimilation in terms of variation of settlement with time. The weighted average of the settlement based on data assimilation was in good agreement with the measured settlement.

Figure 9 shows the probability distribution of the settlement after data assimilation in 2014. The weighted average and standard deviation of the settlement in 2014 were 67.9 and 4.3 cm, respectively. The weighted average was smaller than the field measurement, which was 70.9 cm. The standard deviation was almost equal to that of the observation noise.

Figure 10 shows a comparison between the field measurements and data assimilation in terms of variation of the pore water pressure with time. The weighted average of the pore water pressure at positions No. 3 and No. 8 are in good agreement with the field measurements. Note that the data assimilation could be used to represent the dissipation behavior of the pore water pressure, as shown in Fig. 10(a). However, the pore water pressure obtained from field measurement at position No. 8 was higher than that of the data assimilation, as shown in Fig. 10(c). Moreover, the dissipation rate of the pore

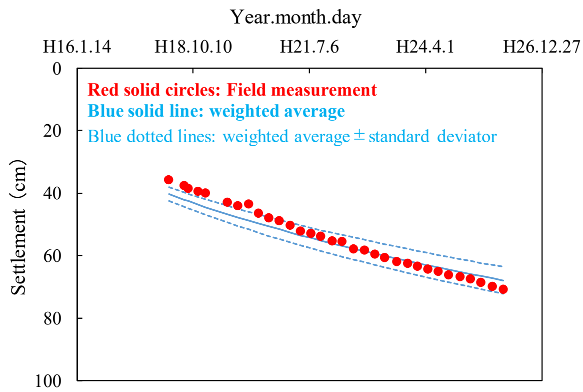

Figure 8. Comparison between field measurements and data assimilation on settlement.

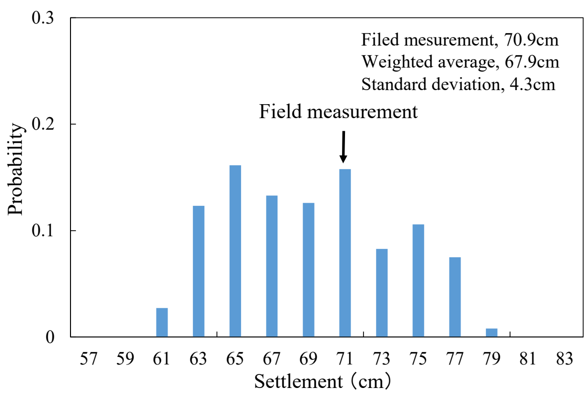

Figure 9. Probability distribution of settlement after data assimilation.

water pressure obtained from the field measurement was slower than that from data assimilation. The dissipation rate of the pore water pressure at position No. 3 was higher than that at position No. 8 from the field measurements. However, the distance between the bottom of the Ma12 layer and the position of the pore water pressure meter at No. 8 was almost equal to that between the upper part of the Ma12 layer and the position of the pore water pressure meter at No. 3. It is suggested that the sand mixed with a gravel layer underneath the Ma12 layer did not quite work as a drainage layer. The boundary condition of the analytical model at the bottom should be modified to perform the appropriate data assimilation.

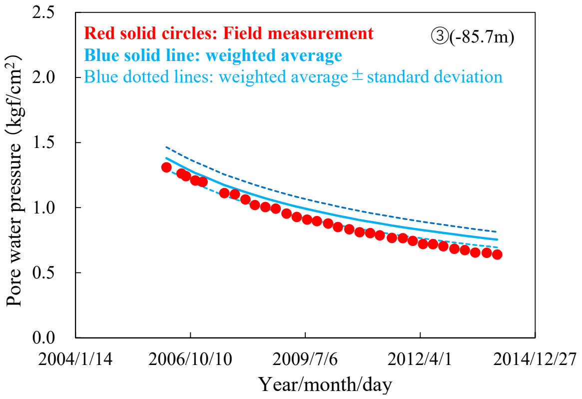

Figure 10(a). Comparison between field measurements and data assimilation on variation of pore water pressure with time (No.3).

Figure 11 shows the vertical distribution of the consolidation parameters determined through data assimilation. The weighted average of consolidation parameters was used as the consolidation parameters. The value of *Cc* determined through data assimilation was almost equal to that of the representative value presented in Fig. 6(a). The expression, *log k*, determined through data assimilation was significantly lower than that of the representative value provided in Fig. 6(b). The *pc* determined through data assimilation was smaller than that of the representative value in Fig. 6(c). It is known that the *pc* of undisturbed clays is considerably influenced by the strain rate. The slower the strain rate, the smaller the *pc* value. The in-situ strain rate was slower than that obtained through consolidation tests in the laboratory owing to the differences in drainage distance in the consolidation tests. Therefore, a difference in *pc* exists in practice. Such a difference was previously discussed based on the field measurements (Hasegawa et al. 2006). It should be noted that the value of *pc*

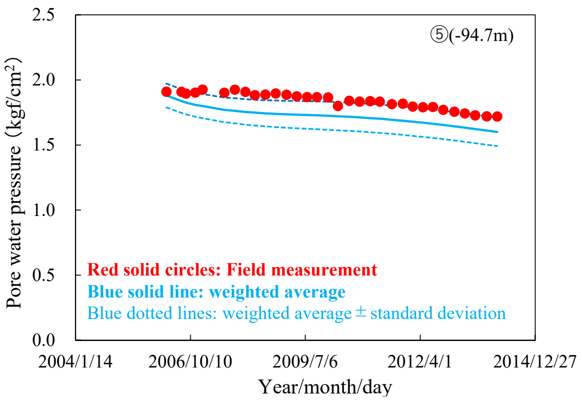

Figure 10(b). Comparison between field measurements and data assimilation on variation of pore water pressure with time (No. 5).

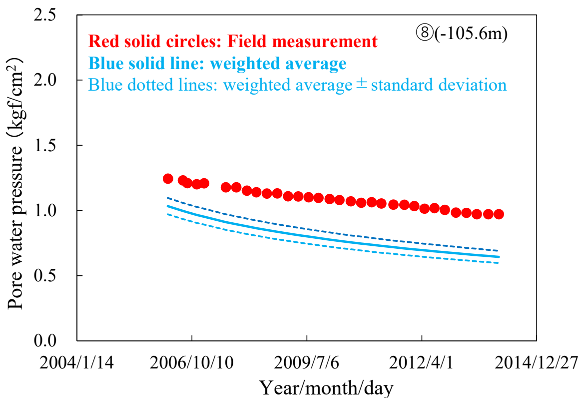

Figure 10(c). Comparison between field measurements and data assimilation on variation of pore water pressure with time (No.8).

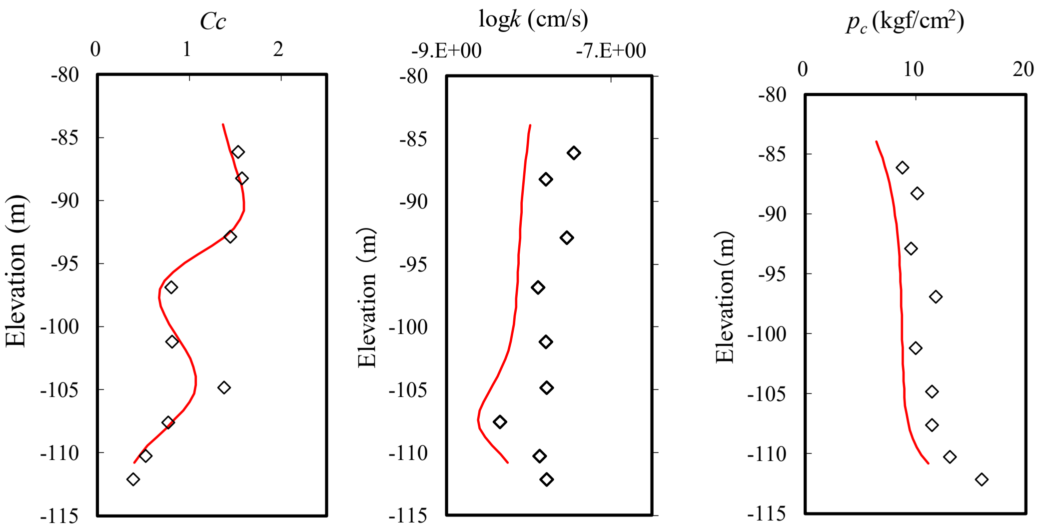

(a) Compression index (b) Coefficient of permeability (c) Consolidation yield stress

Figure 11. Vertical distribution of consolidation parameters determined through data assimilation.

based on field measurements did not increase monotonically with the depth owing to the unevenness of the strain rate in the Ma12 layer. Therefore, a new approach is required for determining the vertical distribution of *pc* before data assimilation.

7. Conclusions

In this study, a simulation model is proposed for reproducing the consolidation behavior of the Ma12 layer using the particle filter method. The main conclusions are summarized as follows.

1. The simulation model could be identified using a particle filter method, even when a simple one-dimensional consolidation analysis with the conventional compression curve composed of two straight lines was applied as a simulation model.
2. The compression index determined through data assimilation was almost equal to that obtained through consolidation tests in the laboratory.
3. The coefficient of permeability determined through data assimilation was significantly less than that determined from consolidation tests in the laboratory.
4. The consolidation yield stress determined through data assimilation was smaller than that obtained in consolidation laboratory tests.
5. The boundary condition of the analytical model at the bottom and the vertical distribution of the consolidation yield stress before data assimilation should be modified to reproduce the consolidation behavior of the Ma12 layer more precisely.

References

Akai, K., and Tamura, T. 1978. Numerical analysis of multi-dimensional consolidation accompanied with elasto-plastic constitutive equation. *Journal of Japan Society of Civil Engineering*, 269: 95-104 (in Japanese).

Futatsugi, S., Nishimura, S., Shuku, T. and Shibata, T. 2018. Evaluation of deformation behavior of a natural slope using elasto-viscoplastic finite element method and observation data. *I.D.R.E Journal*, 306(86-1): II_9-II_18 (in Japanese).

Hasegawa, N., Matsui, T., Tanaka, Y., Takahashi, Y. and Nambu, M. 2006. In-situ consolidation behavior of Pleistocene clay below seabed at Kobe Airport. *Journal of Japan Society of Civil Engineering*, C-62(4): 780-792 (in Japanese).

Ito, S., Oda, K., Koizumi, K., and Usuki, Y. 2016. Identification of soil hydraulic parameters based on in-situ measurements using the particle filter. *Journal of Japan Society of Civil Engineering-C*, 72(4): 354-367 (in Japanese).

Mimura, M., Takeda, K., Yamamoto, K., Fujiwara, T. and Jang, W.Y. 2003. Long term settlement of the reclaimed quasi-overconsolidated Pleistocene clay deposits in Osaka bay. *Soils and Foundations*, 43(6): 141-153.

Shibata, T., Shuku, T., Murakami, A., Nishimura, S. Fujisawa, K., Hasegawa, N. and Nonami, S. 2019. Prediction of long-term settlement and evaluation of pore water pressure using particle filter. *Soils and Foundations*, 59: 67-83.

Shuku, T., Murakami, A., Nishimura, S., Fujisawa, K. and Nakamura. K. 2010. Data assimilation of the settlement behavior of Kobe Airport constructed on reclaimed land using the particle filter. *Journal of Applied Mechanics*, 13: 67-77 (in Japanese).

Tanaka, H. 2005. Consolidation behavior of natural soils around p_c value – Long term consolidation test. *Soils and Foundations*, 45(3): 83-95.

Watabe, Y., Udaka, K. and Morikawa, Y. 2008. Strain rate effect on long term consolidation of Osaka clay. *Soils and Foundations*, 48(4): 495-509.